Analytical solution for the axisymmetric buckling of cylindrical shells

Miguel Lagos & Raj Das

International Journal of Mechanics and Materials in Design

ISSN 1569-1713
Volume 11
Number 2

Int J Mech Mater Des (2015) 11:139-148
DOI 10.1007/s10999-014-9259-9

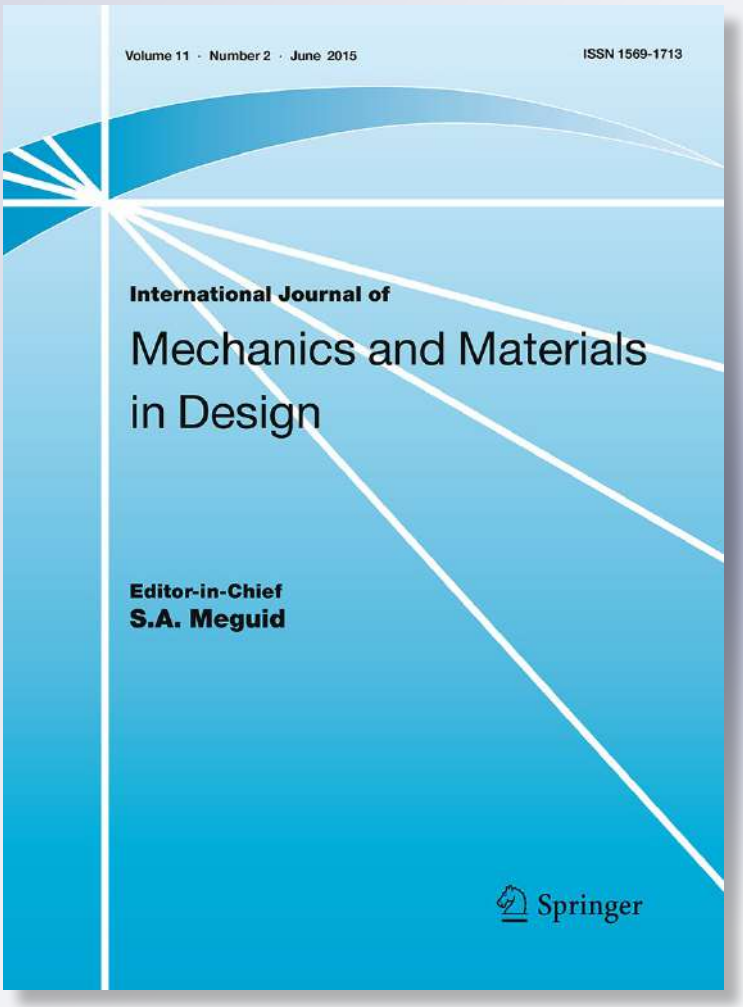

Springer

Int J Mech Mater Des (2015) 11:139–148
DOI 10.1007/s10999-014-9259-9

Analytical solution for the axisymmetric buckling of cylindrical shells

Miguel Lagos · Raj Das

Received: 1 April 2014 / Accepted: 10 May 2014 / Published online: 3 June 2014

Abstract Closed-form analytical solutions for thin shell buckling problem are useful in a wide range of analysis and design problems. In this paper, the profile of a cylindrical shell in the post-buckling regime of axisymmetric deformation is analysed, and the solution is shown to be a Jacobi elliptic sine function, for any load and axial deformation. The exact solution of the non-linear differential equation for the thin elastic shell profile holds for any deformation, up to the limit in which the shell is almost flattened by the applied load. Closed-form expressions are derived also for the load dependent axial deflection and stored energy. The analytical solution of the buckling loads and deformed profile are found to agree well with an equivalent numerical solution. Results show that an axially compressed cylindrical shell exhibits ideal behaviour for a safety shock energy absorber.

Keywords Buckling · Cylindrical shell · Elliptic functions · Energy absorption

M. Lagos · R. Das
Faculty of Engineering, University of Talca, Curicó, Chile
e-mail: mlagos@utalca.cl

R. Das (✉)
Department of Mechanical Engineering, University of Auckland, Auckland, New Zealand
e-mail: r.das@auckland.ac.nz

1 Introduction

Buckling of cylindrical shells is an important problem in mechanics and is commonly encountered in several applications, such as pressure vessels, aerospace and civil structures. Although this system has been a common subject in the specialized literature, only numerical solutions have been reported (Kim and Kim 2002; Hunt et al. 2003; Paschero and Hyer 2009; Pinna and Ronalds 2003; Simitses 1986; Wullschleger and Meyer-Piening 2002). It is envisaged that an analytical solution of this buckling problem will have several advantages in designing thin shell curved structural members. To address this, a closed-form analytical solution for the axisymmetric buckling of an elastic cylindrical shell under an axial load, applied uniformly on its edges, is developed here. Instead of applying directly the methods of the standard theory of elasticity, the present approach resorts to the analysis of the equilibrium of forces at an elementary sector of the shell. Although both procedures are conceptually equivalent, dealing with forces instead of stresses allows for a much simpler derivation of the equation for the shell profile, because forces convey an implicit first integration. In turn, the applied load, shell profile and axial deflection are actually mean values, and hence integrals over the strain fields. The non-linear equation for the buckled axisymmetric thin shell profile can be solved by analytical means and yields a Jacobi elliptic sine function. Closed-form expressions are also derived for the buckling critical load and

energy stored in the post-buckling regime, which yield a complete solution to the problem. Additionally, an exact analytical solution may be useful to validate numerical methods, which can eventually be used to undertake more complex problems.

The analytical solution of this problem constitutes a novel application of the theory of elliptic functions and has importance on practical grounds, for example, in energy absorption devices. A buckling system exhibits the advantages of having a maximum reaction force, the critical load, which can be designed to warrant no damage to the colliding bodies or structures, together with a large energy absorption capability if the geometry is such that the reaction force remains high enough in the post-buckling regime of deformation. For example, dock bumpers in harbours are often designed to work this way.

A cylindrical shell of radius R and axial length L_0, both measured in the unstrained condition, is shown schematically in Fig. 1. The shell thickness e is assumed to be much smaller than the radius R. The applied opposed forces of magnitude P act along the symmetry z-axis and are uniformly distributed on the edges of the cylindrical shell. The material of the cylinder is assumed to be elastic following Hooke's law. Instead of dealing with the model in the most general way, facing all the complex deformation modes a cylindrical shell may display (Kim and Kim 2002; Hunt et al. 2003; Paschero and Hyer 2009; Pinna and Ronalds 2003; Simitses 1986; Wullschleger and Meyer-Piening 2002), the mathematical approach is kept simple by allowing only axisymmetric deformations. Barrel shaped post-buckling deformations constitute an important case (primary deformation mode), but it is well-known that periodic profiles are possible as well (secondary modes).

The mechanical analysis shows that, in a short first stage, the cylindrical shell undergoes a uniform compressive strain along the z-axis, conserving strictly its cylindrical shape and opposing a reaction force proportional to the strain up to a maximal load P_B. The maximum strain reached in this first deformation regime is indicated in Fig. 1a by a discontinuous line. Compression beyond this limit makes the shell to start buckling, and the cylindrical shell progressively acquires a barrel shape, as in Fig. 1b, or a periodic profile. In this second regime the reaction force diminishes monotonically with strain, but always maintaining a significant magnitude. The development

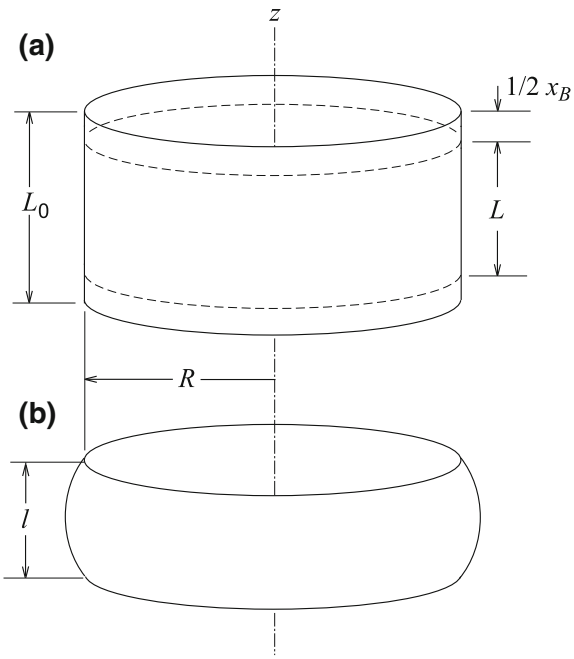

Fig. 1 Schematic view of the cylindrical shell. **a** Unstrained condition (*solid lines*) and critical axial strain for buckling (*discontinuous lines*). **b** Buckled strain regime by the action of compressive axial forces uniformly distributed on the shell edges. Only the fundamental (primary) mode of deformation is shown

of the barrel profile involves stretching of the shell circumference, which requires strong tensile forces that contribute to stabilize the buckled structure. If Young's modulus is the same for tensile and compressive loadings, periodic deformation modes are also possible. The stabilization induced forces along the perimeter of the shell alternate between tension and compression when buckling is periodic.

2 Buckled strain regime of the cylindrical shell of finite thickness

2.1 Equilibrium of the internal forces

Figure 2 shows the cylindrical shell in the strain regime in which it adopts a barrel shaped profile by the axial load P (equivalent to the reaction force at equilibrium, or quasi-equilibrium). The cylindrical coordinate system has its z-axis along the main symmetry axis, and the origin O at the center of the deformed shell, which extends from $z = -l/2$ to $z = l/2$. Distance r is the radius of the shell for a given

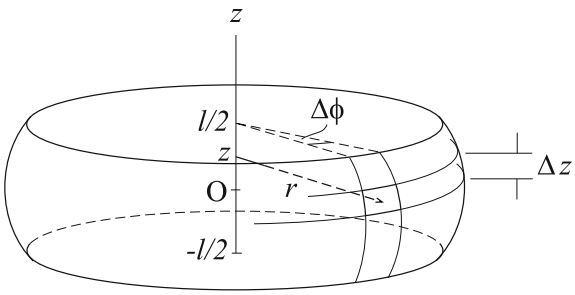

Fig. 2 The deformed cylindrical shell, showing schematically an elementary sector defined by the cylindrical coordinates r, ϕ and z (ϕ is implicit), and by the variations $\Delta\phi$ and Δz

z, so that function $r(z) - R$ determines the profile of the deformed shell. The azimuthal coordinate ϕ is the usual one in cylindrical coordinates, and is not shown in Fig. 2 for the sake of clarity.

The equilibrium equations are derived from the analysis of the forces operating on an elementary sector of the shell, schematically represented in Fig. 2. The method is preferred over simply writing the equations of the theory of elasticity and applying boundary conditions, because it is simpler and provides a better physical insight. The advantages of the procedure are discussed in the final subsection of this section. Figure 2 and the following derivations refer to the fundamental buckling deformation mode to simplify the discussion, however, extension to the general case is straightforward.

Figure 3 displays a diagram of the material element and the forces applied on it. Forces on the plane $\phi = \text{constant}$, containing the z-axis, are compressive forces of magnitude $F_c(z + \Delta z)$ and $F_c(z)$. The forces on the plane $z = \text{constant}$, normal to the z-axis, are tensile forces, because these stretch the shell contour in its plane, and their magnitude is denoted $F_\phi(z)$. Solutions with cylindrical symmetry were implicitly assumed, because the forces were considered to be independent of ϕ. In general, $F_c(z)$ and $F_\phi(z)$ for a thick shell are surface integrals of the components, σ_{ij}, $i, j = r, \phi, z$, of the stress tensor in cylindrical coordinates, which may have a complex dependence on r and z. The analysis on the basis of the equilibrium of forces skips the functional dependence of stress field and remains valid even for thick shells.

Figure 4a is a projection on the plane $z = \text{constant}$ of the system of Fig. 3 showing the forces operating in this plane, and Fig. 4b shows the vector composition of them. Hence, the tensile forces give a sum of magnitude

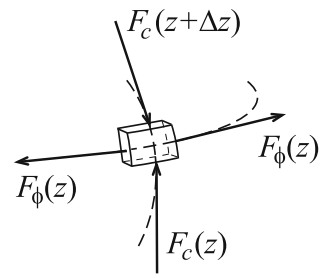

Fig. 3 The elementary sector of Fig. 2 and the compressive and tensile forces F_c and F_ϕ exerted on it

$$2F_\phi(z)\,\sin(\Delta\phi/2) \rightarrow F_\phi(z)\Delta\phi \qquad \text{if } \Delta\phi \approx 0, \tag{1}$$

contained in the plane $z = \text{constant}$ and pointing towards the central z-axis.

Forces in the plane $\phi = \text{constant}$ are shown in Fig. 5. They are the two compressive forces of magnitude $F_c(z + \Delta z)$ and $F_c(z)$ operating in the two opposite edges, and the third one is the resultant of the tensile forces in the plane $z = \text{constant}$, whose magnitude is $F_\phi(z)\Delta\phi$. The former two forces are tangent to the curve $r(z) - R$ determining the shell profile in the corresponding application points, and subtend angles $\theta + \Delta\theta$ and θ with the z-axis, respectively.

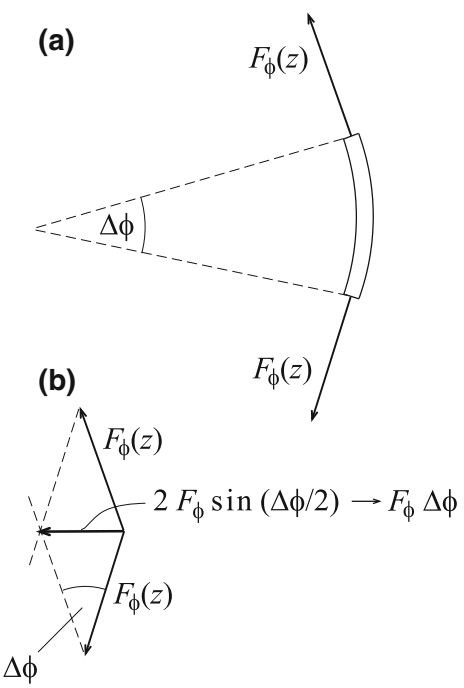

Fig. 4 **a** The graphic scheme of Fig. 3 projected on the plane $z = \text{constant}$. **b** Force diagram in the plane $z = \text{constant}$

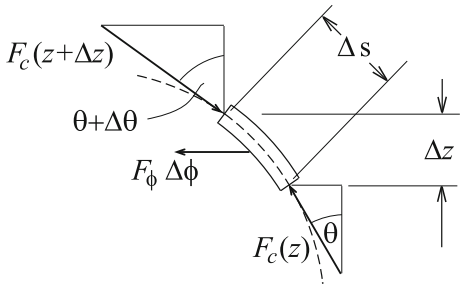

Fig. 5 Forces in the plane $\phi =$ constant. Compressive forces $F_c(z+\Delta z)$ and $F_c(z)$ are tangent to the curve $r(z)$-R representing the shell profile, and subtend angles $\theta+\Delta\theta$ and θ with the z-axis, respectively. The force $F_\phi(z)\Delta\phi$ is obtained in Fig. 4 from the tensile forces in the plane $z =$ constant. The discontinuous line represents the shell profile

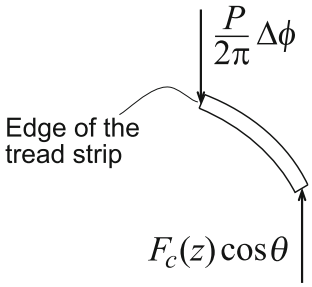

Fig. 6 Equilibrium of a shell fringe of finite size in the z-direction. The z-component $F_c(z)\cos\theta$ of the force is $P\Delta\phi/(2\pi)$ for any z in $[-l/2, l/2]$

Equilibrium requires

$$-F_c(z+\Delta z)\cos(\theta+\Delta\theta)+F_c(z)\cos\theta=0, \tag{2}$$

$$F_c(z+\Delta z)\ \sin(\theta+\Delta\theta)-F_c(z)\ \sin\theta=-F_\phi\Delta\phi. \tag{3}$$

From Eq. (2) one can infer that the z-component of the forces does not depend on z, and hence they can be identified with the external force $P\Delta\phi/(2\pi)$ applied on the edge of the shell fringe defined by $\Delta\phi$. The argument is graphically shown in Fig. 6 and yields

$$F_c(z+\Delta z)\cos(\theta+\Delta\theta)=F_c(z)\cos\theta=\frac{P}{2\pi}\Delta\phi. \tag{4}$$

2.2 Differential equation for the shell profile function $r(z)-R$

Recalling Eq. (4) one can divide the first term in the right hand side of Eq. (3) by $F_c(z+\Delta z)\cos(\theta+\Delta\theta)$, the second one by $F_c(z)\cos\theta$, and the right hand side by $P\Delta\phi/(2\pi)$. It gives

$$\tan(\theta+\Delta\theta)-\tan\theta=-\frac{2\pi F_\phi}{P}. \tag{5}$$

Force F_ϕ can be expressed as

$$F_\phi=\sigma_{\phi\phi}e\Delta s, \tag{6}$$

where $\sigma_{\phi\phi}$ is the normal stress in the azimuthal direction, e is the shell thickness and Δs the length of the shell element shown in Fig. 5, and whose value is

$$\Delta s=\sqrt{1+\left(\frac{dr}{dz}\right)^2}\,\Delta z. \tag{7}$$

Replacing $\tan\theta=-dr/dz$ and combining Eqs. (5), (6) and (7) one obtains that, in the limit $\Delta z\to 0$,

$$\frac{d^2r}{dz^2}=-\frac{2\pi e\sigma_{\phi\phi}}{P}\sqrt{1+\left(\frac{dr}{dz}\right)^2}. \tag{8}$$

On the other hand, the normal stresses σ_{rr}, $\sigma_{\phi\phi}$ and σ_{zz} satisfy Hooke's law

$$\varepsilon_{\phi\phi}=\frac{r-R}{R}=\frac{1}{E}(\sigma_{\phi\phi}-\nu\sigma_{rr}-\nu\sigma_{zz}), \tag{9}$$

where E and ν are the Young's modulus and Poisson ratio of the material the shell is made of. Substituting

$$\sigma_{zz}=-\frac{P}{2\pi re}\cos\theta, \tag{10}$$

$\cos\theta=[1+(dr/dz)^2]^{-1/2}$ and

$$\sigma_{rr}=-\frac{F_\phi\Delta\phi}{r\Delta\phi\Delta z}=-\sigma_{\phi\phi}\frac{e}{r}\sqrt{1+\left(\frac{dr}{dz}\right)^2} \tag{11}$$

in Eq. (9), and solving for $\sigma_{\phi\phi}$, it is obtained that

$$\sigma_{\phi\phi}=\frac{1}{1+\nu\dfrac{e}{r}\sqrt{1+\left(\dfrac{dr}{dz}\right)^2}}\times\left(E\,\frac{r-R}{R}-\frac{\nu P}{2\pi er\sqrt{1+\left(\dfrac{dr}{dz}\right)^2}}\right). \tag{12}$$

Combining Eqs. (12) and (8) one finally obtains

$$\frac{d^2r}{dz^2} = -\frac{\frac{2\pi eE}{RP}(r-R)\sqrt{1+\left(\frac{dr}{dz}\right)^2} - \frac{v}{r}}{1+v\frac{e}{r}\sqrt{1+\left(\frac{dr}{dz}\right)^2}}. \qquad (13)$$

The differential Eq. (13) gives the profile $r(z)$ of the cylindrical shell deformed by the axial load P when the proper physical conditions are imposed to the solutions. The most evident conclusion one can infer from Eq. (13) is that the load P cannot be null. Hence it corresponds to a deformation regime occurring for sufficiently high loads.

The unloaded cylindrical shell has a length L in the axial direction, which reduces to a smaller length l by the applied load P. The length reduction originates from the elastic compressive strain of the deformed shell and by the shape deformation itself projected in the z-direction. If the elastic strain can be neglected when compared to the effect of the shell deformation, the length of the curved path adopted by the deformed shell will conserve its original value L. Hence the physical solutions of Eq. (13) must satisfy

$$L = \int_{-l/2}^{l/2} dz\sqrt{1+\left(\frac{dr}{dz}\right)^2}. \qquad (14)$$

2.3 Present theoretical approach versus theory of elasticity

The equation for the shell profile was derived in the preceding subsections from analysing the equilibrium of the forces exerted on a representative elementary sector of the material medium, introducing from the beginning the symmetry constraints. For our present purposes, this procedure is much simpler and practical than the more standard approach of readily introducing the system boundary conditions into the general formalism of the theory of elasticity. This is because the latter approach oblige us to deal with complex stress distributions, which may not be our main interest. In the theory of elasticity the free surfaces of the shell are defined as surfaces where the stresses vanish, and the theory furnishes the equations for calculating the detailed distribution of the stresses occurring in between. A recent paper by Zozulya and Zhang (2012) provides a good example of this kind of precise calculation of the deformation of cylindrical shells, together with a detailed account of the stress fields inside the material using numerical methods. The cost paid for such a complete solution is the introduction of numerical methods from the very start.

However, if it is not necessary to know about the precise profiles of the outer and inner surfaces of the shell, or how the stresses vary inside, the present approach is quite adequate and provides an exact solution of the deformed profile. The forces $F_c(z)$ and $F_\phi(z)$ in Fig. 3 account for the integrated effect of these stresses, and their equilibrium condition proves to be sufficient for determining the equation for the mean shell profile, which has the advantage of being closed-form.

3 The profile equation for the buckling of a thin shell and its solution

The trivial solution $r =$ constant reduces Eq. (13) to

$$E\frac{r-R}{R} = v\frac{P}{2\pi re} \qquad (r = \text{constant}), \qquad (15)$$

which can be interpreted as the Poisson effect on the shell circular perimeter $2\pi r$ accompanying the uniform axial strain produced by the applied compressive stress $P/(2\pi re)$. This uniform solution, which is expected to be stable up to a critical load P_B, preserves the cylindrical shape and produces only small geometrical variations, because E is usually very large (0.01–500 GPa). The buckled non trivial solutions of Eq. (13) involve much larger deformations. In the post–buckling regime r assumes values in the interval $R < r \leq R + L/2$ when l varies from $l = L$ to $l = 0$. The second term v/r in the numerator of the right hand side of Eq. (13) is comparable with the first one only when $|r-R|/R \ll 1$. As long as r departs from R beyond the range of the purely elastic distortions, the term v/r becomes negligibly small when compared to the one proportional to E. Hence it is advisable to distinguish between elastic strains and geometric changes and write

$$\frac{d^2r}{dz^2} = -\frac{2\pi eE}{PR}(r-R)\sqrt{1+\left(\frac{dr}{dz}\right)^2} \qquad (16)$$

$(\text{buckling, thinshell}).$

Equation (16) also assumes a thin enough shell to neglect the second term in the denominator of the right

hand side of Ec. (13) ($e \ll R$). Although this nonlinear equation is not listed in the specialized treatises on elliptic functions and integrals (Gradshteyn and Ryzhik 2007; Byrd and Friedman 1971), it will be shown next that its exact solution is a Jacobi elliptic sine function, which holds for any load and deformation state, including the limit in which the shell has been completely flattened by the applied force.

Defining

$$y(z) = r(z) - R, \quad p = \frac{2\pi eE}{PR}, \quad R = \text{constant}, \tag{17}$$

Eq. (16) reads

$$y'' = -py\sqrt{1+y'^2}, \tag{18}$$

and the substitution

$$y(z) = \frac{1}{\sqrt{p}}\, u(\sqrt{p}\, z) \tag{19}$$

turns it into

$$u'' = -u\sqrt{1+u'^2}. \tag{20}$$

Multiplying both sides of this equation by u' yields the integrable form

$$\frac{u''u'}{\sqrt{1+u'^2}} = -uu', \tag{21}$$

which can be solved to give

$$\sqrt{1+u'^2} = -\frac{1}{2}u^2 + \frac{1}{2}u_0^2 + 1, \tag{22}$$

where $u_0 = u(0)$. Because of the symmetry with respect to the origin, $u(\sqrt{p}\, z)$ must have its maximum at $z = 0$ and the integration constant was chosen so that $u'(0) = 0$. Denoting now

$$\zeta = \sqrt{p}\, z, \quad v(\zeta) = \frac{u(\zeta)}{u_0}, \quad k^2 = \frac{(u_0/2)^2}{1+(u_0/2)^2}, \tag{23}$$

Eq. (22) can be rewritten as

$$\frac{dv}{d\zeta} = \sqrt{(1-v^2)\left(1 + \frac{u_0^2}{4} - \frac{u_0^2}{4}\, v^2\right)}, \tag{24}$$

or

$$\sqrt{1-k^2}\, \frac{dv}{d\zeta} = \sqrt{(1-v^2)(1-k^2v^2)}. \tag{25}$$

Inverting this equation and integrating with respect to v one has

$$\frac{1}{\sqrt{1-k^2}}(\zeta + \zeta_1) = \int_0^v \frac{dv}{\sqrt{(1-v^2)(1-k^2v^2)}} = F(v,k), \tag{26}$$

where $F(v,k)$ is the incomplete elliptic integral of the first kind with modulus k, $(0 \le k \le 1)$ (Gradshteyn and Ryzhik 2007; Byrd and Friedman 1971), and ζ_1 is an integration constant. The same symbol was used for the integration variable and the upper integration limit to simplify the notation.

The inverse function of the incomplete elliptic integral $F(v,k)$ is known as the Jacobi elliptic sine function sn. Hence Eq. (26) is equivalent to

$$v = \mathrm{sn}\left(\frac{\zeta + \zeta_1}{\sqrt{1-k^2}}, k\right) = \mathrm{sn}\left(\sqrt{\frac{p}{1-k^2}}(z+z_1), k\right). \tag{27}$$

Function $\mathrm{sn}(x,k)$ takes values in the interval $[-1,1]$ and is periodic in x with period $4K(k)$, where $K(k) = F(1,k)$ is the complete elliptic integral of the first kind. Also, $\mathrm{sn}(0,k) = \mathrm{sn}(2K,k) = 0$ and $\mathrm{sn}(K,k) = 1$. The Jacobi sine function is symmetric with respect to $x = K$ and has a maximum there.

Therefore, the solution satisfying the boundary conditions $y(\pm l/2) = 0$ is such that

$$\sqrt{\frac{p}{1-k^2}} = \frac{2K(k)}{l} \quad \text{and} \quad z_1 = \frac{l}{2}. \tag{28}$$

Taking $\sqrt{p}$ and z_1 from these equations, and recalling the third of Eq. (23), which gives $u_0/2 = k/\sqrt{1-k^2}$, one has that the profile of the buckled cylindrical shell is given by

$$y(z) = r(z) - R = \frac{k}{(1-k^2)K(k)}\, \mathrm{sn}\left[\frac{2K(k)}{l}\left(z + \frac{l}{2}\right), k\right]. \tag{29}$$

This solution corresponds to the fundamental (primary) mode of deformation, for which the cylinder takes a barrel shape. As the Jacobi sine function has period $4K(k)$, higher order modes are obtained substituting $(2n+1)K(k)$, with $n = 1, 2, 3, \ldots$, in place of $K(k)$ in Eqs. (28) and (29). Only the fundamental mode will be considered in what follows because the generalization is straightforward.

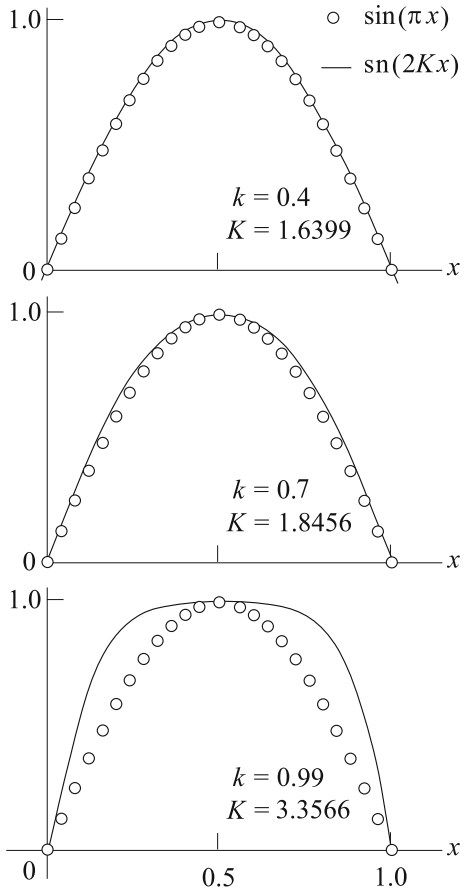

Fig. 7 The Jacobi elliptic sine function (*solid lines*) for three values of the modulus k, compared with the trigonometric sine function (*circles*). For $k<0.7$ the two functions are very similar. At $k > 0.7$ the elliptic function is sensibly broader and goes to a square wave in the limit $k = 1$. Physically, $k = 1$ corresponds to the situation in which the cylindrical shell has been completely flattened by the applied force P and $l = 0$

Combining the first Eq. (28) with the definition (17) of the constant p, a relation between the applied force P and k follows

$$P = \frac{\pi e E l^2}{2R(1-k^2)K^2(k)}. \tag{30}$$

Therefore, it remains just to determine the meaning of k to have a complete solution of our problem. In the next subsection it will be shown that k^2 is essentially the relative axial deformation $\varepsilon = (L-l)/L$ of the cylindrical shell. The elliptic integral $K(k)$ can be calculated quite easily from the defining integral or the series

$$K(k) = \frac{\pi}{2}\left[1 + \sum_{n=1}^{\infty}\left(\frac{(2n-1)!!}{2^n n!}\right)^2 k^{2n}\right]. \tag{31}$$

Figure 7 shows the Jacobi sine function $\mathrm{sn}(2Kx, k)$ for three values of k. The graphs make apparent that the Jacobi elliptic function goes from $\sin(\pi x)$ to a square wave when the modulus k goes from 0 to 1. The latter situation corresponds to the final collapse of the cylindrical shell, when $l = 0$.

3.1 The equation for the modulus k

When $R =$ constant one has $r'(z) = y'(z) = u'(\sqrt{p}\,z)$, hence $(1 + r'^2)^{1/2}$ can be replaced by $(1 + u'^2)^{1/2}$ in the general condition expressed by Eq. (14). Making this and then substituting Eq. (22),

$$L = \int_{-l/2}^{l/2} \sqrt{1+u'^2}\,dz = -\frac{1}{2}\int_{-l/2}^{l/2} u^2(\sqrt{p}\,z)\,dz + \frac{1}{2}u_0^2 l + l. \tag{32}$$

Recalling now

$$u(\sqrt{p}z) = u_0 \,\mathrm{sn}\left[\frac{2K}{l}\left(z+\frac{l}{2}\right), k\right], \quad u_0 = \frac{2k}{\sqrt{1+k^2}}, \tag{33}$$

Eq. (32) can be written as

$$\frac{L-l}{l} = \frac{2k^2}{1-k^2}\left(1 - \frac{1}{2K(k)}\int_0^{2K(k)} \mathrm{sn}^2(\zeta, \mathrm{k})\,\mathrm{d}\zeta\right). \tag{34}$$

The integral appearing in this equation has been solved in terms of the elliptic functions and one has the mathematical identity (Gradshteyn and Ryzhik 2007)

$$\int \mathrm{sn}^2\,\zeta\,d\zeta = \frac{1}{k^2}[u - E(\mathrm{am}\zeta, \mathrm{k})], \tag{35}$$

where $E(\phi, k)$, $0 \le \phi \le \pi/2$, is the second kind incomplete elliptic integral with modulus k. In the usual notation of the theory of elliptic integrals the amplitude am means $\mathrm{am}\,\zeta = \arcsin(\mathrm{sn}\,\zeta)$. Care must be taken in replacing properly the integration limits in the indefinite integral (35) because $0 \le \mathrm{am}\,\zeta \le \pi/2$, and $\mathrm{am}K = \pi/2$. Therefore, $2K$ is outside the domain in which the amplitude function is defined. To overcome this difficulty one can take advantage of

the symmetry of $\mathrm{sn}(x,k)$ with respect to $x = K$ and write

$$\int_0^{2K} \mathrm{sn}^2\zeta d\zeta = 2\int_0^{K} \mathrm{sn}^2\zeta d\zeta = \frac{2}{k^2}[K - E(\pi/2,k)] \tag{36}$$

replacing am $K = \pi/2$. $E(\pi/2,k) = E(k)$ is the complete elliptic integral of the second kind, modulus k, defined by the integral (Gradshteyn and Ryzhik 2007)

$$E(k) = \int_0^{\pi/2} \sqrt{1 - k^2\sin^2\phi}\, d\phi, \tag{37}$$

or the series

$$E(k) = \frac{\pi}{2}\left[1 - \sum_{n=1}^{\infty}\left(\frac{(2n-1)!!}{2^n n!}\right)^2 \frac{k^{2n}}{2n+1}\right]. \tag{38}$$

The term $D(k) = (1/k^2)[K(k) - E(k)]$ can be evaluated either by combining the power series (31) and (38) as

$$D(k) = \frac{K(k) - E(k)}{k^2} = \frac{\pi}{2}\sum_{n=0}^{\infty}\frac{2(n+1)}{2n+1}\left(\frac{(2n+1)!!}{2^{n+1}(n+1)!}\right)^2 k^{2n}, \tag{39}$$

or solving the integral

$$D(k) = \int_0^{\pi/2} \frac{\sin^2\phi\, d\phi}{\sqrt{1 - k^2\sin^2\phi}}, \tag{40}$$

which follows directly from the definitions of $K(k)$ and $E(k)$.

Eq. (34) then becomes

$$\frac{\varepsilon}{1-\varepsilon} = \frac{2k^2}{1-k^2}\left(1 - \frac{D(k)}{K(k)}\right), \quad \varepsilon = \frac{L-l}{L}, \tag{41}$$

which determines exactly the modulus k as a function of only the relative axial compression $\varepsilon = (L-l)/L$. The function $k = f(\varepsilon)$ does not depend on the characteristics of the cylindrical shell and is shown in Fig. 8. The simple approximate rule

$$k^2 \approx \varepsilon \tag{42}$$

holds over the whole range of ε with a 5 % maximum error.

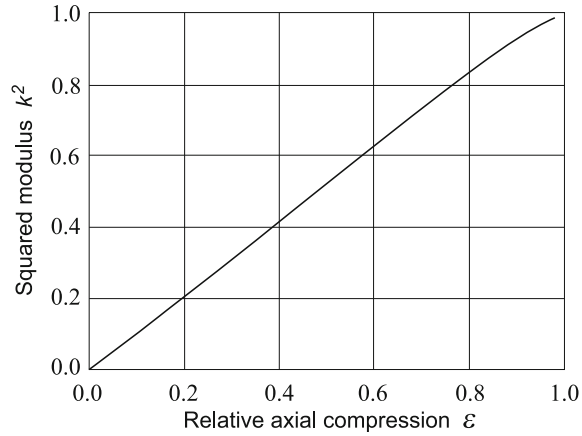

Fig. 8 The squared modulus k^2 and the relative axial compression $\varepsilon = (L-l)/L$, as given by Eq. (41)

4 Critical load, reaction force and energy storage

The deformation regime studied in the preceding sections takes place for a constant non-zero axial load P, given by Eq. (30). This is because it was assumed from the beginning that loading curves the cylindrical shell profile and Eqs. (29), (30) and (41) hold at buckling and in the post-buckling regime of deformation. The variable ε measures only the deformation induced relative displacement of the edges along the axial direction, and the much smaller elastic deformations have been neglected. The force

$$P = \frac{\pi e E L^2(1-\varepsilon)^2}{2R(1-k^2)K^2(k)} \tag{43}$$

has an absolute maximum P_B at $\varepsilon = k = 0$. Recalling $K(0) = \pi/2$, the maximal reaction force reads

$$P_B = \frac{2eEL^2}{\pi R}, \tag{44}$$

and one can write

$$\frac{P(\varepsilon)}{P_B} = \frac{\pi^2}{4}\frac{(1-\varepsilon)^2}{(1-k^2)K^2(k)}. \tag{45}$$

Figure 9 shows P/P_B, which according to Eqs. (45) and (41) is an universal function of ε. Figure 10 shows the energy stored by the shell in the post-buckling deformation regime, obtained integrating Eq. (45) with respect to ε.

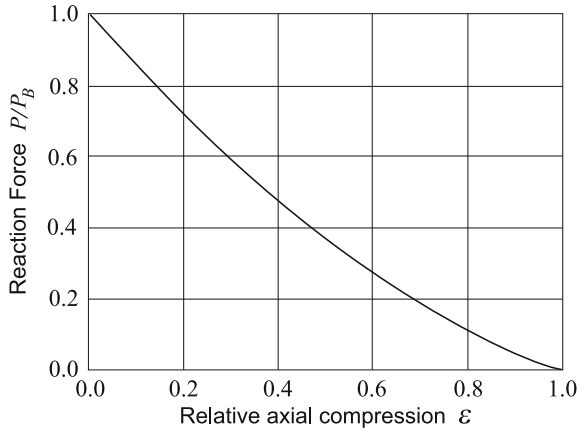

Fig. 9 Reaction force P relative to the maximum P_B as a function of axial compression $\varepsilon = (L - l)/L$, as given by Eq. (45)

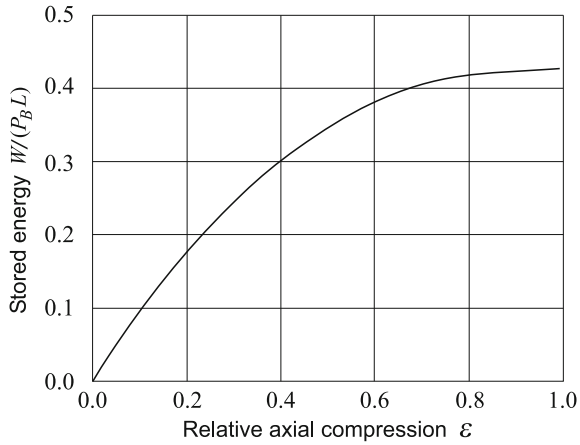

Fig. 10 Energy absorbed by the cylindrical shell in the post-buckling deformation regime, in units of P_BL and for any relative axial compression ε

5 Homogeneous and buckled deformation regimes

The problem focused here is the deformation in which the cylindrical shell is gradually compressed along its main symmetry axis. In a first stage the compression is elastic and conserves the cylindrical shape. The relative displacement x of the edges is given by Hookes's law

$$\frac{P}{2\pi Re} = E\frac{x}{L_0}, \tag{46}$$

where L_0 is the original length of the unstrained cylinder. Once the elastic distortion x takes a critical value x_B, such that the applied force P reaches the threshold value P_B, the cylinder starts to buckle and Eq. (43) starts holding, instead of Eq. (46). At the critical deformation x_B the surface just starts to acquire the barrel shape, and the two deformation regimes coexist. So Eqs. (43) and (46) are both valid for $L = L_0 - x_B$ and $\varepsilon = 0$ (recall that L stands for the shell length when buckling is just initiated). Thus the axial deformation x_B at which the buckling regime sets in can be obtained from combining Eqs. (44) and (46) to eliminate P_B. This yields

$$\frac{x_B}{L_0} = 1 + \left(\frac{\pi R}{\sqrt{2}L_0}\right)^2 - \frac{\pi R}{\sqrt{2}L_0}\sqrt{\left(\frac{\pi R}{\sqrt{2}L_0}\right)^2 + 2}, \tag{47}$$

which is the equation for the critical elastic strain x_B/L_0. Notice that the critical elastic strain x_B/L_0 depends only on the geometric parameters, and not on the mechanical properties of the material. The critical load is

$$P_B = 2\pi ReE\left[1 + \left(\frac{\pi R}{\sqrt{2}L_0}\right)^2 - \frac{\pi R}{\sqrt{2}L_0}\sqrt{\left(\frac{\pi R}{\sqrt{2}L_0}\right)^2 + 2}\right]. \tag{48}$$

6 Comparison with a numerical solution

In this section, we compare the analytical solution developed with the solution of the same problem using a numerical method to assess its consistency with the present analytical solution. To this end, the finite element method (FEM) was used to solve the same problem. The numerical problem considered was the buckling of a thin cylindrical shell under uniform axial compression. The shell had a mean radius of 100 mm and thickness of 5 mm, and Young's modulus was 10 MPa. The cylinder was uniformly compressed by applying a pressure on its edges to initiate buckling. Shell elements were used to mesh the cylinder. A mesh resolution convergence study was performed to ensure that the element size used was of sufficiently fine resolution to produce a highly accurate numerical solution of the buckling problem.

The critical buckling load, P_B, obtained from the numerical solution is 2769 N. This closely compares with that determined from the analytical solution (2666 N), with the difference being 3.7 %. Figure 11 compares the buckled shape (for primary mode) of the cylinder obtained from the present analytical solution

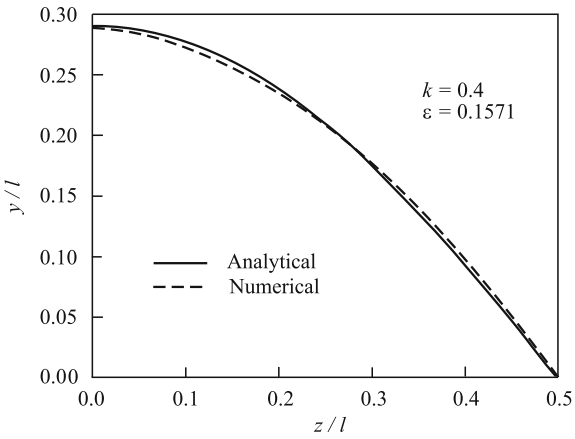

Fig. 11 Comparison of buckled profile of the cylindrical shell, at a buckling stain $\epsilon = 0.1571$ ($k = 0.4$), as obtained by analytical and numerical methods

with that predicted by FEM for the buckling strain of 0.1571 (that corresponds to $k = 0.4$). It is noteworthy that the two shapes agree very well. The load, P, at this configuration as predicted by FEM is 2128 N, which is very close to 2069 N (with the difference being 2.8 %), obtained from the analytical solution. Therefore, the present analytical solution of the cylindrical shell buckling problem is accurate as evaluated against an equivalent fine resolution numerical solution.

7 Conclusions

In this paper, the buckling of cylindrical shells under axial compression is studied. An analytical solution providing the deformed shape of the cylinder in the post-buckling regime is developed. The solution has the advantage of being closed-form, represented by Jacobi elliptic sine function. Such a solution facilitates simple analysis of thin shell structures for bucking without using relatively complex numerical methods, which may require more effort and computer time. An expression for the energy stored by the cylinder is also derived, which can be applied to the design and analysis of energy absorption devices. The present analytical solution is quite accurate as assessed against an equivalent numerical solution. This suggests that the analytical solution can, in turn, be useful to validate the accuracy of various numerical methods for shell buckling problems.

References

Byrd, P.F., Friedman, M.D.: Handbook of Elliptic Integrals for Engineers and Scientists, 2nd edn. Springer, New York (1971)

Gradshteyn, I.S., Ryzhik, I.M.: Table of Integrals, Series, and Products, 7th edn. Academic, Burlington (2007)

Hunt, G.W., Lord, G.J., Peletier, M.A.: Cylindrical shell buckling: a characterization of localization and periodicity. Discret. Contin. Dyn. Syst. B **4**, 505–518 (2003)

Kim, S.-E., Kim, C.-S.: Buckling strength of the cylindrical shell and tank subjected to axially compressive loads. Thin-walled Struct. **40**, 329–353 (2002)

Paschero, M., Hyer, M.W.: Axial buckling of an orthotropic circular cylinder. Application to orthogrid concept. Int. J. Sol. Struct. **46**, 2151–2171 (2009)

Pinna, R., Ronalds, B.F.: Buckling and postbuckling of cylindrical shells with one end pinned and the other end free. Thin-Walled Struct. **41**, 507–527 (2003)

Simitses, G.J.: Buckling and postbuckling of imperfect cylindrical shells: a rewiew. Appl. Mech. Rev. **39**, 1517–1524 (1986)

Wullschleger, L., Meyer-Piening, H.R.: Buckling of geometrically imperfect cylindrical shells-definition of a buckling load. Int. J. Non-Linear Mech. **37**, 645–657 (2002)

Zozulya, V.V., Zhang, Ch.: A high order theory for functionally graded axisymmetric cylindrical shells. Int. J. Mech. Sci. **60**, 12–22 (2012)